



**Preparation and characterization of alginate/chitosan  
formulations for ciprofloxacin controlled delivery**

Journal:	<i>Journal of Biomedical Materials Research: Part B - Applied Biomaterials</i>
Manuscript ID	Draft
Wiley - Manuscript type:	Original Research Report
Date Submitted by the Author:	n/a
Complete List of Authors:	Mazgala, Aleksandra Michna, Justyna Regiel-Futyr, Anna Sebastian, Victor Kyzioł, Agnieszka; Jagiellonian University, Faculty of Chemistry
Keywords:	chitosan, alginate, ciprofloxacin, controlled release

SCHOLARONE™  
Manuscripts

view

1  
2  
3 **Preparation and characterization of alginate/chitosan formulations for ciprofloxacin**  
4 **controlled delivery**  
5

6  
7 **Aleksandra Mazgala<sup>1</sup>, Justyna Michna<sup>1</sup>, Anna Regiel-Futyra<sup>1</sup>, Victor Sebastian<sup>2,3</sup>,**  
8 **Agnieszka Kyzioł<sup>1\*</sup>**  
9

10  
11 <sup>1</sup> Jagiellonian University, Faculty of Chemistry, Ingardena 3, 30-060 Kraków, Poland

12 <sup>2</sup> Department of Chemical Engineering, Nanoscience Institute of Aragon (INA), University of  
13 Zaragoza, 50018 Zaragoza, Spain  
14

15 <sup>3</sup> Networking Research Center on Bioengineering, Biomaterials and Nanomedicine, CIBER-  
16 BBN, 50018 Zaragoza, Spain  
17

18  
19  
20  
21  
22 \*Author for correspondence:

23  
24 Agnieszka Kyzioł, Faculty of Chemistry, Jagiellonian University, 30-060 Cracow, Tel. +48-  
25 12-6632221, Fax: +48-12-6340515, e-mail: [kyziol@chemia.uj.edu.pl](mailto:kyziol@chemia.uj.edu.pl)  
26  
27  
28  
29  
30

31 **Abstract:** In this work, alginate beads loaded with ciprofloxacin (AL\_CP) and alginate  
32 beads loaded with ciprofloxacin and covered by chitosan (AL\_CP\_CS) were prepared by  
33 emulsification technique in combination with internal gelation method. Physicochemical  
34 characterization of the resulting formulations revealed the hydrodynamic diameter and Zeta  
35 potential *ca.* 160 nm and *ca.* -32 mV in case of AL\_CP and *ca.* 240 nm and *ca.* +14 mV in  
36 case of AL\_CP\_CS (pH = 6.0), respectively. Kinetic of ciprofloxacin release from  
37 alginate/chitosan formulations was studied in different media (pH = 1.2, 6.8, and 7.4).  
38 Covering alginate core with a polycation such as chitosan moderates the drug release,  
39 resulting in a pH-sensitive hybrid controlled-release system. Herein, alginate beads with  
40 encapsulated ciprofloxacin covered with chitosan are proposed as an effective oral delivery  
41 system since the drug release from alginate core is limited in low pH solutions (gastric  
42 conditions).  
43  
44  
45  
46  
47  
48  
49  
50

51  
52  
53 **Keywords:** chitosan, alginate, ciprofloxacin, controlled release,  
54  
55  
56  
57  
58  
59  
60

## INTRODUCTION

For the past two decades, biopolymers such as alginate (AL) and chitosan (CS) were the subject of an intense research related to various medical applications, for instance, drug delivery systems,<sup>1-10</sup> materials for regenerative medicine and tissue engineering,<sup>11-16</sup> or even inhibitory materials against biofilm producing bacterial strains.<sup>17</sup>

Alginate is a pH-sensitive, natural, hydrophilic, water-soluble linear polysaccharide isolated from brown sea weeds. It is composed of alternating blocks of  $\beta$ -(1,4)-linked  $\alpha$ -L-guluronic and  $\beta$ -D-mannuronic acid residues. Due to the chelating effect, AL can be cross-linked in the aqueous solution by divalent cations (*e.g.* calcium ions), leading to a facile preparation of hydrogel beads.<sup>12</sup> Various formulations of alginate hydrogels, microspheres, porous scaffolds, and fibers are often selected as supporting matrix for the entrapment and delivery of DNA or RNA, proteins (*e.g.* immunoglobulin G),<sup>7</sup> genes, drugs (*e.g.* ciprofloxacin, doxorubicin, carboplatin, isoniazid, rifampicin, pyrazinamide, ethambutol, *etc.*),<sup>1,18,19</sup> vaccines,<sup>20</sup> enzymes, growth factors or living cells for tissue engineering.<sup>1,21</sup> Alginate typically forms nanoporous gels with a pore size of  $\sim 5$  nm assuring rapid diffusion of encapsulated drugs.<sup>12</sup> Depending on the site of implantation, biomaterials fabricated from alginate are subjected to different pH environments, which affect their degradation properties such as mechanical properties, swelling behavior, the drug release kinetics. Higher molecular weight (MW) decreases the number of reactive positions available for hydrolysis, which further facilitates a slower degradation rate.<sup>11</sup> The anionic character of alginate in solution allows for electrostatic interactions with positively charged small molecules or other polymers such as chitosan, leading to ionic gelation and thus formation of nanoparticulated formulations.

Chitosan is a typical cationic linear polysaccharide, which is obtained by the N-deacetylation of chitin. CS is composed of randomly distributed  $\beta$ -(1,4)-linked D-glucosamine and N-acetyl-D-glucosamine units.<sup>22</sup> This mucoadhesive biopolymer can easily encapsulate drug molecules with a high loading efficiency and form nano- and microparticles in aqueous media. A typical non-covalent ionic cross-linking process enabling for nanoparticles formation can be realized by association with negatively charged multivalent ions such as tripolyphosphate (TPP).<sup>17,23</sup> This physically reversible way of cross-linking overcomes the possible toxicity of covalently bonded reagents such as glutaraldehyde. Pioneering work of Calvo *et al.* explored the potential of pharmaceutical applications of chitosan as a drug carrier.<sup>24</sup> So far, chitosan has been proposed for delivery of proteins, enzymes (*e.g.* lysozyme)<sup>25</sup> or drugs (*e.g.* ciprofloxacin).<sup>26</sup>

Both AL and CS are well-known mainly due to their biocompatibility, biodegradability, non-antigenicity, nontoxicity under the normal physiological conditions, muco- and bioadhesiveness as well as mild gelation conditions.<sup>1,2,11,27</sup> AL/CS nano- and micro-formulations have been recently proposed as drug delivery systems for DNA,<sup>28,29</sup> proteins (e.g. bovine serum albumin,<sup>21</sup> insulin,<sup>2,5,8,30</sup> hemoglobin<sup>10</sup>), oligonucleotides (e.g. epidermal growth factor receptor (EGFR) antisense),<sup>31</sup> drugs (e.g. ampicillin,<sup>3</sup> enoxaparin<sup>6</sup>), enzymes (e.g.  $\beta$ -galactosidase),<sup>32</sup> and cells<sup>33,34</sup>.

Ciprofloxacin (CP) is a second-generation quinolone causing bacterial death by effective inhibition of DNA gyrase and topoisomerase IV.<sup>35</sup> CP is an antibiotic commonly associated with gastric and intestinal problems when administrated orally. However, it is also commonly used across Europe for the cystic fibrosis (CF) treatment.<sup>19</sup> To reduce its toxicity and strong undesirable side effects (i.e. arthritis damage for children with CF) resulting from long-term application, various drug delivery systems such as microcapsules, gels, liposomes, *etc.* have been proposed so far.<sup>36-38</sup>

In this study, biopolymeric formulations based on alginate/chitosan containing ciprofloxacin for sustainable delivery of this antibiotic are presented. Biopolymers, AL and CS, were selected to develop a composite core-shell matrix. Kinetics of ciprofloxacin release from well-characterized alginate/chitosan formulations were studied in different pH conditions: (i) simulating gastric fluid (pH = 1.2), (ii) simulating intestinal fluid (pH = 6.8), and (iii) phosphate buffer saline (pH = 7.4). The developed system is proposed as a promising delivery carrier to treat chronic infection with *Pseudomonas aeruginosa* and to reduce the viscoelasticity of the mucus accumulated into the intestine of cystic fibrosis patients.

## MATERIALS AND METHODS

### Chemicals

Polymers: sodium alginate and chitosan from the chitin of shrimp shells (average molecular weight (MW):  $360 \pm 1$  kDa, deacetylation degree (DD):  $81 \pm 2$  %)<sup>39</sup> were purchased from *Sigma-Aldrich* and used without any further purification. Ciprofloxacin, calcium carbonate, calcium chloride, acetic acid, paraffin oil, Span 80, Tween 80, were also supplied by *Sigma-Aldrich* and all were of analytical grade. Phosphate-buffered saline (PBS, pH = 7.4) was purchased from ALAB (Poland).

Sodium alginate (2% w/v, stock) and chitosan (1% w/v, stock) were dissolved in deionized water and 0.1 M acetic acid respectively during overnight stirring at 65°C.

## Preparation procedure

### *Preparation of alginate beads*

Ciprofloxacin-loaded alginate beads (AL\_CP) were prepared by adopting the method of Silva *et al.* based on emulsification/internal gelation with some modifications.<sup>10</sup> A suspension of ultrafine CaCO<sub>3</sub> or both CaCO<sub>3</sub> and ciprofloxacin in alginate solution was homogenized in an ultrasonic bath for 15 min (620 W, 50 Hz). Then, the mixtures were dispersed in paraffin oil containing a lipophilic surfactant Span 80 (1% v/v) as an emulsion stabilizing agent. The mixtures were stirred vigorously for 15 min. Next, glacial acetic acid was added to the water/oil emulsion and stirring was continued for the next 30 min to provide the alginate pH reduction to approximately 5.0, which permits solubilization of CaCO<sub>3</sub> and ciprofloxacin (pK<sub>a</sub> = 6.09).<sup>40</sup> This allows for efficient cross-linking of alginate core. Beads dispersed in oil phase were recovered by washing with a washing media (CaCl<sub>2</sub> (0.05 M), Tween 80 (1% v/v), pH = 6.3). The suspension was centrifuged for 5 min at 5000 rpm. All supernatants were collected for determination of the unloaded ciprofloxacin concentration. The particles were re-suspended in washing media and procedure was repeated three times.

### *Preparation of alginate/chitosan formulations*

Freeze-dried alginate cores loaded with ciprofloxacin were coated with chitosan, by subsequent cross-linking with sodium tripolyphosphate (TPP, 10 mg/ml). In brief, chitosan (5 mg/ml) was added dropwise to the previously dispersed in distilled water AL\_CP formulation (10 mg/ml). The mixture was stirred for 10 min and then TPP was added dropwise. Cross-linking was carried out for the next 30 min. Weight ratio of AL:CS:TPP was usually 1:2:2, if not indicated differently as 8:4:1, 4:4:1, 1:2:4 or 1:2:1. Finally, after chitosan cross-linking, the core-shell beads (AL\_CP\_CS) were washed twice with deionized water to remove the uncrosslinked chitosan and the cross-linking agent leftovers.

AL\_CP and AL\_CP\_CS were frozen and lyophilized (Alpha 1-2 LD plus, Christ) with or without cryoprotectant (sucrose, 10 % (w/w))<sup>41</sup> at 0°C for 18 h. The obtained particles were stored at 4°C before further use.

## Materials characterization

Fourier transform-infrared (FT-IR) spectra of lyophilized and un-lyophilized samples were obtained using an IR spectrophotometer with attenuated total reflection (ATR-IR, Perkin-Elmer). The spectra were recorded in the 4000-400 cm<sup>-1</sup> range with 1 cm<sup>-1</sup> step. The size was

determined by nanoparticles tracking analysis with NanoSight LM10-HS (Malvern Instruments, The Netherlands). The zeta potential ( $\zeta$ ) was measured using Zetasizer Nano ZS instrument (Malvern Instruments, The Netherlands). The freeze-dried beads were suspended in an aqueous medium at room temperature and sonicated before the measurements. Data were analyzed using the Malvern software and the average values were calculated from at least five separate measurements. All the experiments were performed in triplicate for independent particles batches. Shape and size of the obtained beads were studied by scanning electron microscopy (NOVA NanoSEM 200, FEI).

### ***Loading efficiency***

The ciprofloxacin loading efficiency (LE) was evaluated by an indirect spectrophotometric method *via* measuring absorbance at 277 nm corresponding to the maximum absorption peak of the antibiotic. The unloaded ciprofloxacin in all collected supernatants was determined by assessing its losses during preparation and recovery. The concentration of ciprofloxacin was calculated from a calibration curve. Antibiotic loading (%) was determined from the difference between the initial amount of drug and the total losses. In brief, LE(%) was calculated by the following equation (1):

$$LE(\%) = \frac{T-F}{T} \times 100\% \quad (1)$$

where T and F are respectively total and free amount of ciprofloxacin. The total amount of drug was recognized as an initial concentration of CP in the synthesis solution. The free CP concentration was calculated according to the calibration curve equation.

### ***Cumulative drug release profiles***

The cumulative drug release (CDR) experiments were carried out by suspending the beads in 20 ml of the desired medium at a final concentration of 1 mg/ml in 25 ml flasks. The flask was incubated at a required temperature of 37°C and equipped with a magnetic stirrer. At the predetermined time intervals, 400  $\mu$ l release medium was taken out and the fresh medium with the same volume was added to the flask to maintain the unchanged volume. The amount of ciprofloxacin released from the beads was determined at 277 nm with a UV-Vis spectrometer after the previous separation from the beads by centrifugation (5000g/5 min). The data are presented as the average value of at least three independent experiments.

Simulated gastric fluid (SGF, pH = 1.2) and simulated intestinal fluid (SIF, pH = 6.8 and 7.4) were prepared as described in US Pharmacopoeia (USP 26, 2000).<sup>42</sup>

### *Statistical analysis*

All experiments were repeated at least three times for independent particle batches. Data are presented as mean values  $\pm$  standard deviation (SD).

## **RESULTS AND DISCUSSION**

### **Preparation of alginate/chitosan beads loaded with ciprofloxacin**

Polysaccharide-based systems are nowadays expected to open new possibilities for the drug delivery platforms. The formulations proposed in this paper belong to a novel class of hybrid systems that in addition to one biopolymeric cross-linked core (*i.e.* AL) comprise an additional polysaccharide shell (*i.e.* CS). Such systems present improved physicochemical properties such as better stability in biological media and sustainable pharmacological profiles of drug release.<sup>8,43</sup>

Several different physicochemical factors are governing particles absorption by cells. It is well-known that hydrophobic, negatively charged particles smaller than 1  $\mu\text{m}$  exhibit the best absorption rate due to occurring endocytosis and phagocytosis. However, the uptake strongly depends as well on the type of the treated cells.<sup>44</sup> Furthermore, chitosan is of a great interest for nanoparticulated oral delivery systems since it is able to reduce the transepithelial electrical resistance and transiently opening tight junction between epithelial cells.<sup>45</sup> In general, following intravenous injection, drug-loaded particles can be rapidly cleared from the blood by the mononuclear phagocyte system (MPS), involving the macrophages of the liver, the spleen, and the circulating monocytes. In most cases, the more hydrophobic the surface of the particle is, the more rapid is its uptake from circulation. However, this can be also modulated by the particle size and the other physicochemical surface properties. Even if alginate formulations exhibit properties avoiding the uptake, such as hydrophilicity and an electronegative surface<sup>11</sup>, covering the core by chitosan results in a positively charged core-shell structure that favors immediate opsonization by serum proteins. This ensures a higher rate of cellular uptake, compared to negatively charged systems. However, on the other hand, complexation of the positively charged particles with DNA or other electronegative compounds present in cell environment can reduce the cytotoxicity of the initial polycations towards cells of healthy tissue.<sup>21</sup>

Herein, alginate/chitosan core-shell beads were prepared by emulsification with internal gelation technique as a carrier system for delivery of a model drug, ciprofloxacin (CP). Firstly, drug-loaded alginate core was fabricated by mixing the drug and polymer with an

1  
2  
3 organic emulsion under constant vigorous stirring. Chitosan shell was formed as a result of  
4 the interaction between the negatively charged sodium alginate and the positively charged  
5 chitosan.<sup>46</sup> It is known that low molecular weight chitosan forms a thick shell better anti-  
6 swelling ability compared with chitosans of higher MW.<sup>47</sup> For this reason, chitosan with low  
7 MW was chosen for this study.  
8  
9

10  
11 Since according to literature the optimal pH for the formation of a polyelectrolytic  
12 complex between AL and CS is *ca.* 4.5, this pH was maintained during covering process. This  
13 pH value seems to be the most favorable for the interaction between chitosan and alginate as  
14 the  $pK_a$  of the chitosan is around 6.5 and the  $pK_a$  of the sodium alginate is between 3.4 and  
15 4.4.<sup>48,49</sup> Also other authors postulate pH of 4.6 – 4.8 as the optimal conditions for AL\_CS  
16 synthesis.<sup>50</sup>  
17  
18

19  
20 In detail, the formation of alginate core loaded with ciprofloxacin is occurring by  
21 ionotropic gelation of AL with  $Ca^{2+}$ . Thus, the second important factor influencing AL\_CS  
22 synthesis is a concentration of calcium ions, which are significant elements for building and  
23 maintenance of AL\_CS formulations structure. Calcium ions bind to the carboxylic groups of  
24 alginate and form a gelled net called “egg box”.<sup>10,50</sup> In the applied synthesis reducing the pH  
25 of the alginate solution to *ca.* 5.0 by adding acetic acid permits  $CaCO_3$  solubilization.  
26 Importantly,  $CH_3COOH$  to  $CaCO_3$  molar ratio determines the degree of alginate gelation.  
27 This, in turn, affects the spheres’ mean size. In the next step, polyelectrolyte complexation  
28 with CS takes place. It is known that the negatively charged  $-COO^-$  groups of the alginate  
29 create the intermolecular linkages with the positively charged  $-NH_3^+$  of the chitosan under  
30 defined pH conditions.<sup>2</sup> In addition, in the presence of TPP, it is expected that the ionic  
31 gelation process occurs through the complexation of the  $P_3O_{10}^{5-}$  and  $HP_3O_{10}^{4-}$  groups of TPP  
32 with CS’s  $-NH_3^+$  groups. It was proved by Ko *et al.* that crosslinking process occurs the most  
33 efficiently in the acidic solutions, since in low pH only  $P_3O_{10}^{5-}$  anions exist, which interact  
34 with positively charged groups of chitosan.<sup>4</sup>  
35  
36  
37  
38  
39  
40  
41  
42  
43  
44  
45  
46  
47

#### 48 **Particles size and surface morphology**

49  
50 Chitosan/alginate beads loaded with ciprofloxacin (AL\_CP\_CS) were prepared with  
51 varying volume and molecular ratios of reagents. The best possible formulations were  
52 prepared with  $V_{H_2O}/V_{paraffin}$  ratio = 0.4,  $n_{CH_3COOH}/n_{CaCO_3}$  ratio = 2.5, 2.0 mg/ml AL, 4.4 mg/ml  
53 CS and 80 mg CP, demonstrated a mean hydrodynamic diameter of  $158 \pm 33$  nm and  
54  $239 \pm 27$  nm for AL\_CP and AL\_CP\_CS, respectively, as measured by NTA (FIGURE 1).  
55  
56  
57  
58  
59  
60



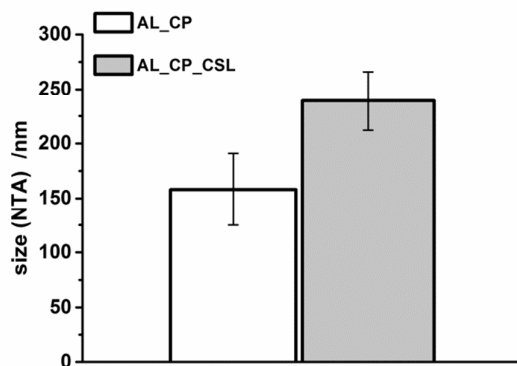


**FIGURE 1.** The mean hydrodynamic diameter determined by NTA for AL\_CP and AL\_CP\_CS formulations.

For successful drug delivery, the particles have to be characterized by high loading efficiency (LE). During preparation of the core/shell beads, pH was maintained around 4.5 allowing the most efficient formation of alginate-chitosan complex due to increased ionic interactions between the carboxyl groups in the alginate and the protonated amine groups in the chitosan. Formation of the dense polymeric layer through chitosan cross-linking with TPP assures the increased entrapment of ciprofloxacin and reduces the leakage of the drug. The average efficiency of ciprofloxacin loading in AL\_CP\_CS formulations was calculated to be  $74.6 \pm 8.51\%$  ( $n = 10$ ).

SEM analysis confirmed the AL\_CP and AL\_CP\_CS particles to be spherical with solid dense structure (FIGURE 2). The size distribution of the particles based on the micrographs was obtained with ImageJ software (more than 100 particles was counted).

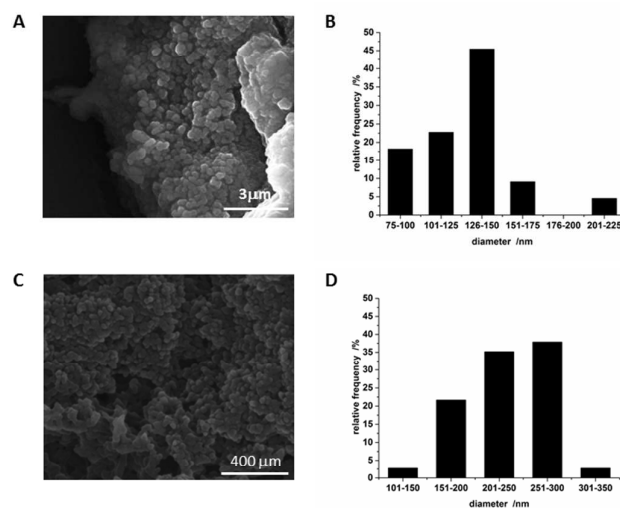


**FIGURE 2.** SEM image of the AL\_CP (A) and AL\_CP\_CS (C) particles with the corresponding size distribution (ImageJ) for AL\_CP (B) and AL\_CP\_CS (D), respectively.

The average size of the resulting AL\_CP and AL\_CP\_CS particles was  $166 \pm 21$  nm and  $252 \pm 21$  nm, respectively. In general, the size estimated from SEM images is in agreement with size obtained from NTA analysis.

In addition, the mean hydrodynamic diameter of the obtained particles increased slightly after the freeze-drying process (data not shown). This is a direct consequence of particle aggregation during the drying process.<sup>51</sup> Therefore, to overcome this problem the use of sucrose as a cryoprotectant was tested at various concentrations. Finally, sucrose concentration of 10 % (w/w) was chosen.

The zeta potential has a considerable influence on (i) the stability of colloidal systems, (ii) the interactions of nanoparticles with other charged molecules, (iii) the adhesion of a drug delivery system onto biological surfaces, and (iv) the efficiency of the synthesis steps (directly related to the establishment of electrostatic interactions), *etc.*. In general, the larger value of the particle zeta potential, the more stable is colloidal system. Particles with the  $\zeta > \pm 30$  mV are considered as moderate stable. On the contrary, the colloidal system tends to agglomerate when the particles zeta potential has too small value. The latter with zeta potentials between 5 and 15 mV is considered to exhibit limited flocculation.<sup>52</sup>

AL\_CP particles showed a negative value of  $-32.0 \pm 1.4$  mV in pH = 6.0, which assures the moderate stability of the particle suspensions in water and in tested buffers (*vide infra*).

Whereas, AL\_CP\_CS particles had a positive surface potential around +14 mV (pH = 6.0; Figure 3A). The inclusion of CS in the AL\_CP\_CS system leads to the observed inversion of  $\zeta$ -potential to a positive value, what reflects the presence of the positively charged  $-\text{NH}_3^+$  groups of chitosan exposed on the surface and unambiguously confirms the presence of a chitosan shell. On the other hand, the presence of AL in the system results in a significant reduction in  $\zeta$  value with respect to the CS-TPP particles, which is reported to be even  $\sim +40$  mV at pH *ca.* 6.<sup>26</sup> Our results are in agreement with Zhang *et al.* and Mukhopadhyay *et al.* who have reported the Zeta potential of chitosan particles cross-linked with TPP to be +16.7 mV<sup>5</sup> and +16.42 mV<sup>8</sup>, respectively. The low  $\zeta$  value of the resulting AL\_CP\_CS particles may be explained by ineffective core covering with chitosan or the possibility of chitosan penetration into the alginate core during the formation process. It may be also explained by the formation of AL\_CS blended particles with a homogeneous distribution of both polymers inside the spheres.<sup>2,5</sup> Since in our experimental system alginate cores were prepared separately and they were lyophilized before chitosan covering, therefore it is supposed that the formed compact surface of alginate- $\text{Ca}^{2+}$  effectively prevents chitosan molecules from penetration into the AL core.

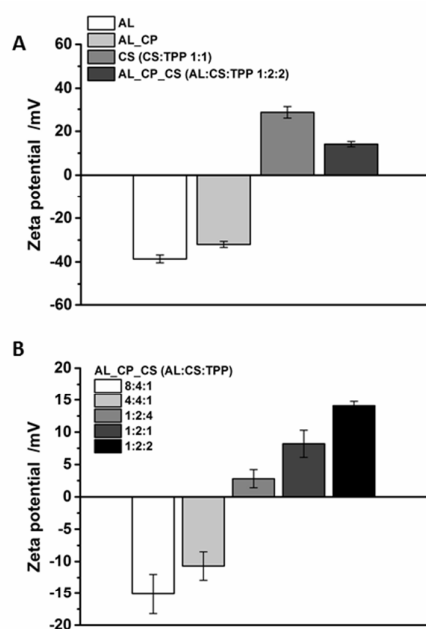


**FIGURE 3.** Zeta potential dependency on formulation content (A) and the weight ratio of particular polymers and TPP (B) in pH = 6.0.

Zeta potential of the resulting formulations was also examined in terms of the different mass ratio of particular polymers and TPP (Figure 3B). Firstly, with the increasing ratio of CS/AL, the Zeta potential value inversion was observed. The higher content of CS the more positive charge was determined varying from  $+15.1 \pm 3.1$  mV and  $+14.1 \pm 0.7$  mV for AL:CS:TPP mass ratio 8:4:1 and 1:2:2, respectively. Secondly, in the case of the AL\_CP\_CS formulation, the increasing content of cross-linker the higher positive  $\zeta$  value was examined. Both observed effects confirm that the most stable AL\_CP\_CS particles are possible to be formed in the case of the double chitosan excess in respect to the alginate and with the mass ratio CS:TPP equal 1:1.

In addition, since both alginate and chitosan are organic matrixes, it is difficult to distinguish them in the SEM and TEM images and confirm core-shell structure by these techniques. Therefore, the formation of AL/CS spheres was undoubtedly confirmed by a detailed FTIR analysis (FIGURE 4).

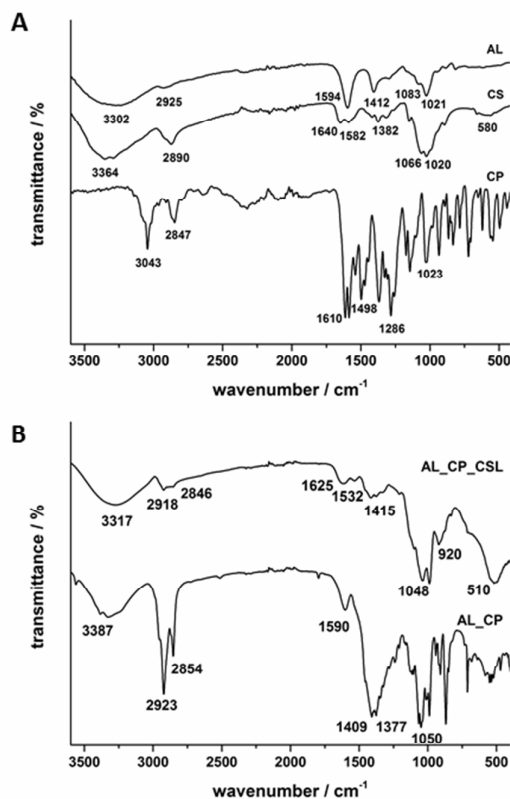


**FIGURE 4.** FTIR spectra of AL, CS, and CP (A), and AL\_CP and AL\_CP\_CS (B).

1  
2  
3 In the infrared spectrum of AL characteristic peaks at  $\sim 1594\text{ cm}^{-1}$  and  $\sim 1412\text{ cm}^{-1}$  were  
4 assigned to the asymmetric and symmetric stretching vibrations of the unreacted  $-\text{COOH}$   
5 groups. A broad band around  $1021\text{ cm}^{-1}$  was attributed to the saccharide structure of AL (C-  
6 O-C stretching).<sup>8</sup> The spectrum of CS revealed a characteristic band in the region  $3400-$   
7  $3200\text{ cm}^{-1}$ , attributed to  $-\text{NH}_2$  and  $-\text{OH}$  groups stretching vibrations and the amide I band at  
8  $1640\text{ cm}^{-1}$ .<sup>8,18,48</sup> The characteristic absorption peaks at  $1286\text{ cm}^{-1}$  and  $1610\text{ cm}^{-1}$  of  
9 ciprofloxacin, obtained in the AL\_CP\_CS spectrum, appeared due to the stretching vibration  
10 of C-F bond and the vibration of phenyl framework conjugated to  $-\text{COOH}$ , respectively.  
11 Furthermore, the stretching vibrations of C-H in the phenyl framework were observed at  
12  $3043\text{ cm}^{-1}$  and  $2845\text{ cm}^{-1}$ .<sup>53</sup> It can be clearly seen that the latter characteristic bands shifted to  
13  $2923\text{ cm}^{-1}$  and  $2854\text{ cm}^{-1}$  in the case of AL\_CP, and to  $2918\text{ cm}^{-1}$  and  $2846\text{ cm}^{-1}$  in the case of  
14 AL\_CP\_CSL. It confirmed that CP was encapsulated in the polymeric matrix.

15  
16 Moreover, in the FTIR spectrum of AL\_CP\_CS, the asymmetrical and symmetrical  
17 stretching of  $-\text{COO}^-$  groups of untreated AL were shifted to  $1625\text{ cm}^{-1}$  and  $1415\text{ cm}^{-1}$ ,  
18 respectively. Likewise, the absorption band at  $1625\text{ cm}^{-1}$  can be also attributed to the shifted  
19 band of CS from  $1640\text{ cm}^{-1}$ . In the spectra of the AL\_CP\_CS core-shell particles, broadening  
20 of the band observed at approximately  $3317\text{ cm}^{-1}$  may be assigned to the hydrogen bonds  
21 between chitosan and sodium alginate. Furthermore, a new peak at  $1532\text{ cm}^{-1}$  assigned to the  
22 alginate carboxylic groups interacting with chitosan was detected. These results confirm the  
23 carboxylic groups of AL association with the ammonium groups of CS through electrostatic  
24 interactions and thus formation of the polyelectrolyte complex.<sup>29</sup> The observed band shifts  
25 from  $3302\text{ cm}^{-1}$  (AL) to  $3387\text{ cm}^{-1}$  (AL\_CP) and from  $3364\text{ cm}^{-1}$  (CS) to  $3317\text{ cm}^{-1}$   
26 (AL\_CP\_CS) were also most likely caused by interactions between AL with CP and CS.  
27 While C-H vibrations of AL at  $2925\text{ cm}^{-1}$  and CS at  $2890\text{ cm}^{-1}$  were probably overlapped by  
28 vibration of C-H of phenyl framework of CP. All these observations proved that the model  
29 antibiotic was efficiently encapsulated in the polymeric matrix and amine groups of CS  
30 interact with the carboxylic groups of AL forming the self-assembled particles.

### 31 32 33 34 35 36 37 38 39 40 41 42 43 44 45 46 47 48 49 50 51 **Cumulative drug release profiles**

52 Drug molecules, from small chemical drugs to macromolecular proteins, can be released  
53 from the polymeric formulations in a controlled manner, depending on the cross-linker type  
54 and applied cross-linking methods. In addition, alginate/chitosan formulations can be orally  
55 administrated or injected into the body in a minimally invasive manner, which allows  
56  
57  
58  
59  
60

1  
2  
3 extensive applications in the pharmaceutical arena.<sup>12</sup> However, an important and necessary  
4 condition prior to successful *in vivo* implementation is an in-depth knowledge of the loaded  
5 drug release kinetics and mechanisms.  
6  
7

8 During alginate-Ca beads preparation the loose network of beads may cause leakage of  
9 the drug through the pores. This is a major limitation of such systems, however, covering  
10 alginate beads with a polycation such as a chitosan significantly improves their mechanical  
11 properties and reduces permeability. The complexation process moderates the porosity and  
12 results in the diminished leakage of the encapsulated drug.<sup>8,46,50</sup> What is noteworthy, such  
13 hybrid systems exhibit a pH-sensitivity. Alginate beads with encapsulated drug and covered  
14 with chitosan can be proposed for oral delivery systems since the drug release from alginate  
15 beads is reduced in low pH solutions.<sup>5,45,54</sup> For instance, chitosan/alginate beads were  
16 originally designed for the protection of protein macromolecules (*e.g.* insulin) from the  
17 aggressive environment of the stomach, when this poorly absorbable drug is administered  
18 orally. An encapsulated drug is partially retained in a gastric pH environment (pH = 1.2),  
19 while a more extensive release is observed under intestinal pH simulation (pH = 6.8).<sup>55,56</sup> In  
20 the case of cystic fibrosis treatment, ideally CP should not be released in gastric pH, whereas  
21 a slow release within 3 to 5 hours should occur in intestinal fluid.<sup>10</sup>  
22  
23  
24  
25  
26  
27  
28  
29  
30

31 In our experimental system, the release of ciprofloxacin from AL\_CP and AL\_CP\_CS  
32 formulations was carried out in media of different pH at conditions corresponding to the  
33 gastric (pH = 1.2, SGF) and intestinal (pH = 6.8, SIF and pH = 7.4, PBS) body fluids, at 37°C  
34 (Figure 5-7). Firstly, cumulative drug release (CDR) was examined in water (pH *ca.* 6.0) in  
35 terms of different polymer content of the resulting formulations. Three types of formulations:  
36 CS\_CP, AL\_CP and AL\_CP\_CS were investigated (Figure 5).  
37  
38  
39  
40  
41  
42  
43  
44  
45  
46  
47  
48  
49  
50  
51  
52  
53  
54  
55  
56  
57  
58  
59  
60

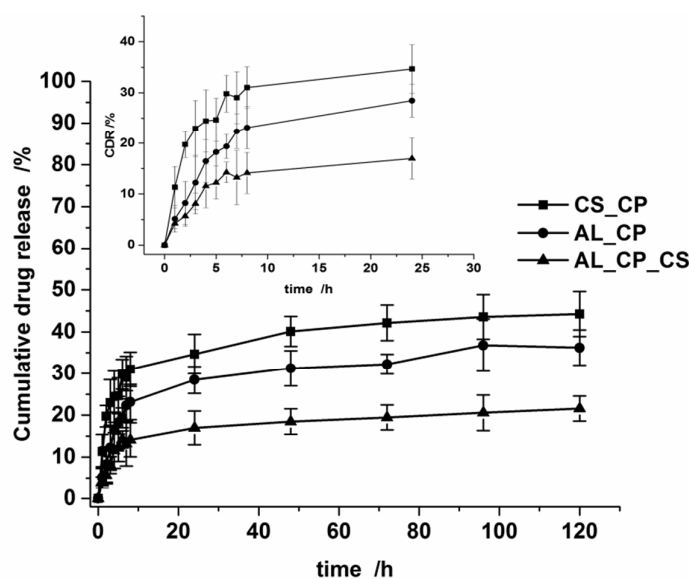


**Figure 5.** Kinetic curves of ciprofloxacin release over time in aqueous media at 37°C from the CS\_CP (■), AL\_CP (●), and AL\_CP\_CS (▲) formulations. Inset: magnification of release time scale (from 0 to 24 hours).

The obtained CDR profiles were characterized by an initial “burst effect” (Figure 5, inset) followed by a continuous and controlled release in the case of all studied formulations. It was revealed that the rate of ciprofloxacin release for the core-shell AL\_CP\_CS was the slowest, reaching  $21.6 \pm 3.0\%$ , while in the case of CS\_CP value of CDR was estimated to be  $44.2 \pm 5.4\%$ , after 120 hours of the experiment. This indicates that the hybrid formulation (AL\_CP\_CS) significantly limits release of the encapsulated antibiotic in the studied media. At this pH, close to the  $pK_a$  of chitosan, rapid and efficient drug release was not observed in the case of AL\_CP\_CS particles, even though the alginic core in these conditions is totally converted to a soluble salt of sodium alginate. This can be ascribed to insoluble chitosan shell, which prevents the ciprofloxacin release.

Then, the release of ciprofloxacin from AL\_CP\_CS formulations was carried out in conditions corresponding to the gastric (pH = 1.2, SGF) and intestinal (pH = 6.8, SIF and pH = 7.4, PBS) body fluids. All of the releasing experiments were conducted at 37°C under constant stirring conditions (Figure 6).

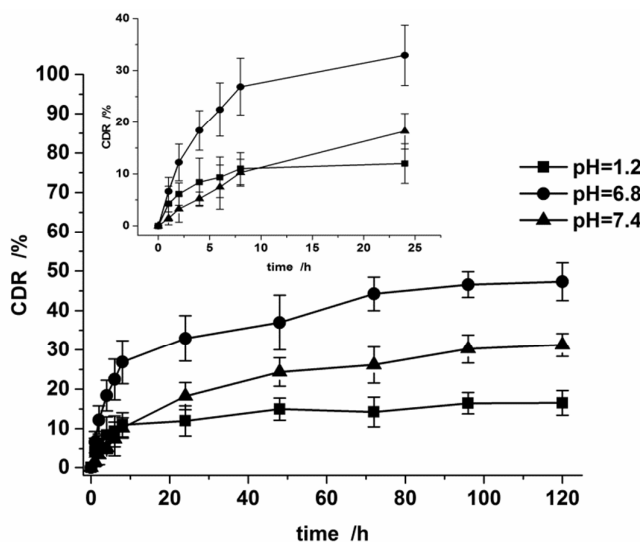


**FIGURE 6.** Kinetic curves of ciprofloxacin release over time from the AL\_CS\_CP formulations in different pH = 1.2 (■), pH = 6.8 (●), and pH = 7.4 (▲) at 37°C. Inset: magnification of release time scale (from 0 to 24 hours).

When weak ions, such as AL and CS, are involved in polyelectrolytic complexes, the number of electrostatic linkages is a function of pH, due to changes in the dissociation degree of the polyelectrolytes.<sup>57</sup> In an acidic medium (pH = 1.2), alginate is protonated, while calcium alginate matrices are depleted of calcium ions. This results in a conversion to insoluble alginic acid forming a tight network, which displays swelling properties with the low release characteristics. However, this treatment significantly reduces the gel strength favoring the drug release by diffusion. Moreover, in this conditions, chitosan is in a soluble form and the polymer shell may follow a slow erosion, what results in observed slow drug release by diffusion ( $16.5 \pm 3.1$  %; 120 h). At pH = 6.8 although, the alginic acid is formed and is converted into a soluble sodium alginate salt, the entire antibiotic release was not observed. This indicates that the AL\_CS\_CP beads structure is still preserved, mainly because of the presence of partially insoluble in this conditions chitosan shell. The other explanation of poor drug release ( $47.3 \pm 4.8$  %; 120 h) can be the strong charge interactions between ciprofloxacin's carboxylic groups, which are gradually deprotonated with increased pH and can combine with positively charged chitosan. However, with increasing pH deprotonation of chitosan also progresses, what makes such interactions more and more impossible. Thus, the treatment of the AL\_CS\_CP formulations in the increasing pH causes a significant weakening of the interactions inside the shell and between core and shell, as well. On the other hand, at pH = 7.4, resembling neutral pH of blood plasma, which is suitable for antimicrobial activity



1  
2  
3 testing, only *ca.* 30% of CDR was detected after 120 hours of releasing. This can be explained  
4 by the fact that unionized chitosan shell does not favor the swelling and the matrix erosion, as  
5 well as the drug diffusion. Thus, chitosan shell effectively provides the control over the drug  
6 release.  
7  
8

9  
10 In can be concluded that at the acidic pH polyelectrolytic complex of CS and AL swells  
11 less, while more at pH values above 6.5, since it is the  $pK_a$  of CS. At low pH CS is  
12 protonated, what is exhibited by the formation of  $-NH_3^+$  groups, whereas AL possesses its  
13 carboxylic groups in non-ionized form ( $-COOH$ ) with a tendency to precipitate.<sup>49,50,58</sup> This  
14 can result in a tightly closed structure and a strong control over the drug release. Thus, the  
15 swelling properties reflect in the ionization of the studied polyelectrolytes and in consequence  
16 in the kinetics of drug release. In general, the rate of drug release depends on numerous  
17 factors and primarily is an interplay between a complexes structure of the studied  
18 formulations and the impact of the resultant ions and their charges in a given pH. Moreover,  
19 what is noteworthy, the other crucial parameters that affect the release rate of a drug from the  
20 studied hybrid formulations is the composition of the releasing media.<sup>26</sup> Pure water does not  
21 screen so effectively the charge interactions between both alginate and chitosan core-shell as  
22 well as alginate core and antibiotic. Consequently, the release rate in such media as SIF and  
23 PBS buffers is significantly higher than in pure water. This is also attributed to the exchange  
24 of calcium(II) with sodium ions (present in buffer media) leading to the disintegration of  
25 calcium alginate core.<sup>15</sup> As well, in both SIF and PBS buffers other possible ions interactions  
26 between polymer polyelectrolytes and ions existing in buffers may significantly influence  
27 cumulative drug release profiles.  
28  
29  
30  
31  
32  
33  
34  
35  
36  
37  
38

39  
40 To study the release kinetics, the experimental data obtained from drug release studies in  
41 different pHs were plotted in various kinetic models: (i) zero order: CDR(%) *vs.* time; (ii) first  
42 order:  $\log(CDR(\%)_{\text{remaining}})$  *vs.* time; (iii) Higuchi model: CDR(%) *vs.* square root of time; (iv)  
43 Hixson-Crowell: cube root of  $CDR(\%)_{\text{remaining}}$  *vs.* time; and (v) Korsmeyer-Peppas:  
44  $\log(CDR(\%))$  *vs.*  $\log(\text{time})$ .<sup>43,54,59</sup> The correlation coefficients of the release profiles,  
45 calculated according to different mathematical models for the analysis of the release kinetics,  
46 were summarized in Table 1.  
47  
48  
49  
50  
51  
52  
53  
54  
55  
56  
57  
58  
59  
60

**TABLE 1** Correlation coefficients for different mathematical models applied on the release kinetics from the AL\_CS\_CP formulations in different pHs.

Kinetic model	Correlation coefficient ( $R^2$ ) <sup>a</sup>		
	pH = 1.2	pH = 6.8	pH = 7.4
Zero order	0.9412	0.9489	0.9841
First order	0.9462	0.9645	0.9840
Higuchi	<b>0.9856</b>	<b>0.9910</b>	0.9713
Hixson-Crowell	0.9446	0.9596	0.9841
Korsmeyer-Peppas (n) <sup>b</sup>	<b>0.9894</b> (0.44)	0.9778 (0.64)	<b>0.9892</b> (0.89)

<sup>a</sup> Bold values indicate the best fits

<sup>b</sup> Release exponent (n) evaluated for <60% of drug release

Zero order kinetics, the cumulative amount of drug released versus time, describes concentration-independent drug release rate from the formulation. Whereas, first order, presented as log cumulative percent drug remaining versus time, describes concentration-dependent drug release from the system. Then, Higuchi's model, which is a cumulative percentage of drug released versus square root of time, describes the release of drug based on Fickian diffusion as a square root of the time-dependent process from the swellable insoluble matrix. This is the case of pH = 6.8, for which the best linearity was found in Higuchi's equation plot ( $R^2 = 0.9910$ ). Apparently, in this pH chitosan shell provides an insoluble barrier to drug diffusion. Then, Hixson-Crowell cube root law, the cube root of percentage drug remaining versus time, correlated the release from systems with polymer erosion/dissolution resulting in a change in surface area and diameter of particles. Surprisingly, although this kinetic model should be an appropriate one for the studied polymeric formulation, none fitting turned to be the best. Lastly, by incorporating the first 60% of release data mechanism of release can be indicated according to Korsmeyer where n is the release exponent, indicative of mechanism of drug release. In the case of ciprofloxacin releasing in pH = 1.2, the release exponent was calculated to be  $n = 0.44$ . This indicates release mechanism according to Fickian diffusion law. While, in the case of higher pHs the release exponents were calculated to be  $n = 0.64$  and  $n = 0.89$  for pH = 6.8 and pH = 7.4, respectively. This indicates that in the first case, the release mechanism is by non-Fickian diffusion, while in the second case kinetics is similar to the zero-order kinetics (case II transport).<sup>60,61</sup> Case-II relaxational release is the drug transport mechanism associated with stresses and state-transition in hydrophilic polymers which swell in water or biological fluids.

In conclusion, the mechanism of drug release from polymer-based matrices is complex and not completely understood. Presumably, drug release follows more than one type of mechanism. In the case of release from the surface, what may occur in the case of AL\_CP beads, drug adsorbed on the surface dissolves instantaneously when it comes in contact with the release medium. This may occur when chitosan shell becomes totally dissolved in acidic conditions resembling the gastric fluids (pH = 1.2) and the beads are transferred into simulated intestinal body fluids (pH = 6.8). The early phase of the release corresponds to the release of drugs physically bound to the surface and the delayed phase due to the release of entrapped drug due to diffusion of the drug from the rigid matrix structure. In our experimental case, ciprofloxacin is probably released both by diffusion and by erosion mechanism. Certainly, the disintegration of the beads is pH-dependent and the release medium content effectively influences the drug release (*vide supra*).

Finally, in order to obtain data on the behavior of alginate/chitosan beads during the gastrointestinal passage, the release of ciprofloxacin was studied in the simulated gastric fluid (SGF) in pH of 1.2 for the first 2 hours. Then the medium was replaced with the simulated intestinal fluid (SIF) and release was performed for the next 48 hours in pH of 6.8 (Figure 7).

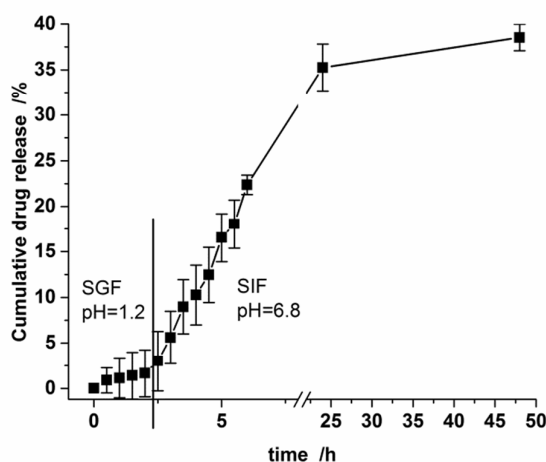


**FIGURE 7.** The kinetic curve of ciprofloxacin release over time from the AL\_CS\_CP formulations firstly in pH = 1.2 and then continued in pH = 6.8 at 37°C.

Sequential release experiment simulating the gastrointestinal tract has proved pH-sensitive release patterns, not only protecting the studied drug in the acidic environment of the stomach but as well controlling its release in the intestinal tract. After first 2 hours of treatment in pH = 1.2 presumably CS shell is disintegrating and the gel strength of AL core

1  
2  
3 beads is reduced, however, the antibiotic release is prevented since detected CDR value was  
4 *ca.* 2%. After changing pH to a higher value, the -COOH groups of AL are converted to -  
5 COO<sup>-</sup> resulting in the formation of soluble sodium alginate. As well, with an increase of pH  
6 the electrostatic repulsion can increase because of the secondary amine group in piperazine  
7 ring of CP. All these resulted in increased drug release shown by CDR values of  $47.3 \pm 4.8\%$ .  
8  
9

10  
11 In conclusion, in our experimental system, beads prepared without chitosan shell  
12 (AL\_CP) were generally characterized by the faster kinetics of drug release, when compared  
13 with alginate/chitosan hybrid materials (AL\_CP\_CSL). This was mainly because of an  
14 additional barrier provided by chitosan. Moreover, chitosan under this condition of  $\text{pH} > 6.5$   
15 is insoluble, what explains a slow release of ciprofloxacin from AL\_CP\_CSL in  $\text{pH} = 7.4$   
16 ( $24.3 \pm 3.6$  after 48 hours, Figure 6). The situation is totally different when AL\_CP\_CSL  
17 beads are firstly incubated in low pH (SGF,  $\text{pH} = 1.2$ ) (Figure 7). In this case, the observed  
18 low value of CDR can be explained by a tight alginate network formed at low pH. Then, after  
19 transfer to more neutral pH of SIF (6.8), the hydroxyl ions will tend to displace the anionic  
20 alginate. This will result in losing of the positive charge by chitosan, dissociation of the  
21 alginate-chitosan complex and finally lead to matrix erosion. Moreover, the influence of low  
22 pH is not negligible on mechanical properties of beads and may cause the reduction in the gel  
23 strength after acidic treatment, what in turn may result in enhancement of drug release in the  
24 second stage of release under higher pH conditions. Indeed, a study on the simulation of the  
25 tract leading to the systematic circulation from the gastrointestinal environments after oral  
26 delivery of the drug revealed that ciprofloxacin release is hindered in acidic pH of the  
27 stomach and then stable and sustained drug retention in intestinal media is allowed.  
28  
29  
30  
31  
32  
33  
34  
35  
36  
37  
38  
39  
40

## 41 CONCLUSIONS

42  
43 In this work, ciprofloxacin-loaded biopolymeric systems based on alginate/chitosan  
44 formulations for sustainable delivery of the antibiotic are presented. Spherical AL\_CP and  
45 AL\_CP\_CS beads with the diameter *ca.* 160 nm and 240 nm, respectively were synthesized  
46 according to the modified procedure combining emulsification and internal gelation methods.  
47 AL\_CP particles exhibited a negative value of Zeta potential (*ca.* -32 mV,  $\text{pH} = 6.0$ ), while  
48 AL\_CP\_CS particles were characterized by a positive surface electrokinetic potential around  
49 +14 mV at the same pH conditions. In-depth analysis of the releasing profiles revealed pH-  
50 dependent kinetics. An initial “burst effect” was observed in simulated gastrointestinal fluids  
51 ( $\text{pH} = 1.2$  and 6.8), and in phosphate buffer solution ( $\text{pH} = 7.4$ ), followed by a continuous and  
52  
53  
54  
55  
56  
57  
58  
59  
60

1  
2  
3 controlled release phase. In the lowest pH, the drug release mechanism is due to Fickian  
4 diffusion, while in the case of the higher pHs due to anomalous non-Fickian transport  
5 (pH = 6.8) and case II transport (zero order kinetics; pH = 7.4). Chitosan shell provides an  
6 effective barrier hindering drug release, what was proved in sequential release experiment  
7  
8  
9  
10  
11  
12  
13  
14  
15  
16  
17  
18  
19  
20  
21  
22  
23  
24  
25  
26  
27  
28  
29  
30  
31  
32  
33  
34  
35  
36  
37  
38  
39  
40  
41  
42  
43  
44  
45  
46  
47  
48  
49  
50  
51  
52  
53  
54  
55  
56  
57  
58  
59  
60

controlled release phase. In the lowest pH, the drug release mechanism is due to Fickian diffusion, while in the case of the higher pHs due to anomalous non-Fickian transport (pH = 6.8) and case II transport (zero order kinetics; pH = 7.4). Chitosan shell provides an effective barrier hindering drug release, what was proved in sequential release experiment simulating the gastrointestinal tract. Studied hybrid biopolymeric formulations can be proposed as a promising delivery systems to treat, for instance, chronic bacterial infections in case of cystic fibrosis patients, since the structure of these formulations can be preserved in acidic conditions of the stomach and the release of antibiotic can be facilitated later in the digestive tract.

### ACKNOWLEDGEMENTS

This work was supported by Foundation for Polish Science within POMOST project “Alginate/chitosan core-shell beads with bioactive functionalities” (POMOST/2013-7/7). The research was also carried out with the equipment purchased thanks to the financial support of the European Regional Development Fund in the framework of the Polish Innovation Economy Operational Program (contract no. POIG.02.01.00-12-023/08).

### REFERENCES

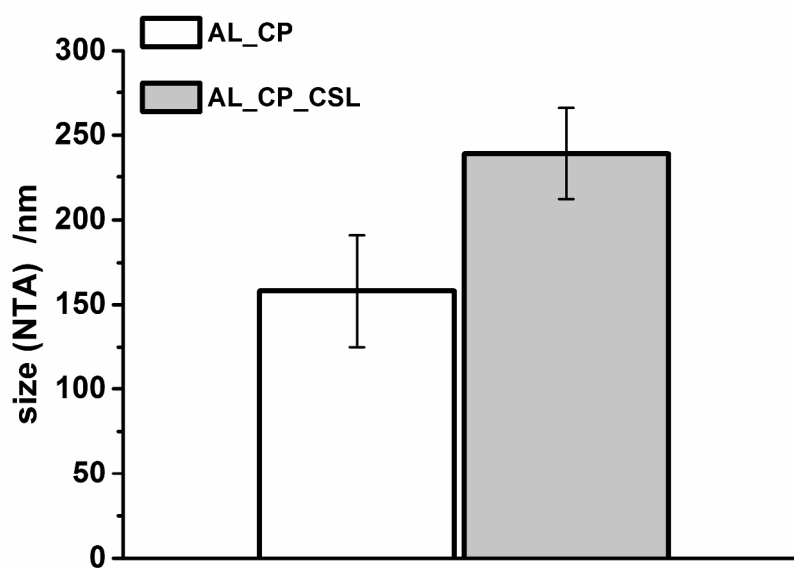
1. Li Y, Maciel D, Rodrigues J, Shi X, Tomas H. Biodegradable Polymer Nanogels for Drug/Nucleic Acid Delivery. *Chem. Rev.* 2015;115:8564–8608.
2. Goycoolea FM, Lollo G, Remunan-Lopez C, Quaglia F, Alonso MJ. Chitosan-Alginate Blended Nanoparticles as Carriers for the Transmucosal Delivery of Macromolecules. *Biomacromolecules* 2009;10(7):1736-1743.
3. Anal AK, Stevens WF. Chitosan–alginate multilayer beads for controlled release of ampicillin. *International Journal of Pharmaceutics* 2005;290:45-54.
4. Ko JA, Park HJ, Hwang SJ, Park JB, Lee JS. Preparation and characterization of chitosan microparticles intended for controlled drug delivery. *International Journal of Pharmaceutics* 2002;249:165-174.
5. Zhang Y, Wei W, Lv P, Wang L, Ma G. Preparation and evaluation of alginate–chitosan microspheres for oral delivery of insulin. *European Journal of Pharmaceutics and Biopharmaceutics* 2011;77(1):11-19.
6. Bagre AP, Jain K, Jain NK. Alginate coated chitosan core shell nanoparticles for oral delivery of enoxaparin: *in vitro* and *in vivo* assessment. *Int J Pharm* 2013;456:31-40.
7. Zhai P, Chen XB, Schreyer DJ. Preparation and characterization of alginate microspheres for sustained protein delivery within tissue scaffolds. *Biofabrication* 2013;5:1-11.
8. Mukhopadhyay P, Chakraborty S, Bhattacharya S, Mishra R, Kundu PP. pH-sensitive chitosan/alginate core-shell nanoparticles for efficient and safe oral insulin delivery *Int J Biol Macromol* 2015;72:640-648.
9. Shu XZ, Zhu KJ. Controlled drug release properties of ionically cross-linked chitosan beads: the influence of anion structure. *International Journal of Pharmaceutics* 2002;233:217-225.

10. Silva C, Ribeiro A, Figueiredo M, Ferreira D, Veiga F. Microencapsulation of hemoglobin in chitosan-coated alginate microspheres prepared by emulsification/internal gelation. *The AAPS Journal* 2005;7(4):E903-E913.
11. Sun J, Tan H. Alginate-Based Biomaterials for Regenerative Medicine Applications. *Materials* 2013;6:1285-1309.
12. Lee KY, Mooney D, J. Alginate: Properties and biomedical applications. *Progress in Polymer Science* 2012;37:106- 126.
13. Ziani K, Henrist C, Jerome C, Aqil A, Mated JI, Cloots R. Effect of nonionic surfactant and acidity on chitosan nanofibers with different molecular weights. *Carbohydrate Polymers* 2011;83(2):470-478.
14. Bhattarai N, Li Z, Edmondson D, Zhang M. Alginate-based nanofibrous scaffolds: structural, mechanical and biological properties. *Advances Materials* 2006;18:1463-1467.
15. Chang JJ, Lee JH, Wu MH, Yang MC, Chien CT. Preparation of electrospun alginate fibers with chitosan sheath. *Carbohydrate Polymers* 2012;87:2357- 2361.
16. Hu WW, Yu HN. Coelectrospinning of chitosan/alginate fibers by dual-jet system for modulating material surfaces. *Carbohydrate Polymers* 2013;95:716-727.
17. Machul A, Mikołajczyk D, Regiel-Futyr A, Heczko PB, Strus M, Arruebo M, Stochel G, Kyzioł A. Study on inhibitory activity of chitosan-based materials against biofilm producing *Pseudomonas aeruginosa* strains. *Journal of Biomaterials Applications* 2015;30:269-278.
18. Parveen S, Mitra M, Krishnakumar S, Sahoo SK. Enhanced antiproliferative activity of carboplatin-loaded chitosan-alginate nanoparticles in a retinoblastoma cell line. *Acta Biomaterialia* 2010;6:3120-3131.
19. Islan GA, Bosio VE, Castro GR. Alginate Lyase and Ciprofloxacin Co-Immobilization on Biopolymeric Microspheres for Cystic Fibrosis Treatment. *Macromol. Biosci.* 2013;13:1238-1248.
20. Borges O, Cordeiro da Silva A, Romeijn SG, Amidi M, de Sousa a, Borchard G, Junginger HE. Uptake studies in rat Peyer's patches, cytotoxicity and release studies of alginate coated chitosan nanoparticles for mucosal vaccination. *Journal of Controlled Release* 2006;114:348-358.
21. Schutz CA, Juillerat-Jeanneret L, Kauper P, Wandrey C. Cell Response to the Exposure to Chitosan-TPP/Alginate Nanogels. *Biomacromolecules* 2011;12:4153-4161.
22. Krajewska B. Application of chitin- and chitosan-based materials for enzyme immobilization: a review. *Enzyme and Microbial Technology* 2004;35:126-139.
23. Jonassen H, Kjøniksen AL, Hiorth M. Stability of Chitosan Nanoparticles Cross-Linked with Tripolyphosphate. *Biomacromolecules* 2012;13:3747-3756.
24. Calvo P, Remunan-Lopez C, Vila-Jato JL, Alonso MJ. Novel hydrophilic chitosan-polyethylene oxide nanoparticles as protein carriers. *J. Applied Polym. Sci.* 1997;63:125-132.
25. Lian ZX, Ma ZS, Wei J, Liu H. Preparation and characterization of immobilized lysozyme and evaluation of its application in edible coatings. *Process Biochemistry* 2012;47:201-208.
26. Liu H, Gao C. Preparation and properties of ionically cross-linked chitosan nanoparticles. *Polym. Adv. Technol.* 2009;20:613-619.
27. Sonia TA, Sharma CP. Chitosan and Its Derivatives for Drug Delivery Perspective. *Adv. Polym. Sci.* 2011;243:23-54.
28. Quong D, Neufeld RJ. DNA protection from extracapsular nuclease, within chitosan-or poly-l-lysine -coated alginate beads. *Biotechnol. Bioeng.* 1998;60:124-134.
29. Douglas KL, Tabrizian M. Effect of experimental parameters on the formation of alginate-chitosan nanoparticles and evaluation of their potential application as DNA carrier. *Journal of Biomaterials Science -- Polymer Edition* 2005;16(1):43-56.
30. Reis CP, Ribeiro AJ, Veiga F, Neufeld RJ, Damge C. Polyelectrolyte Biomaterial Interactions Provide Nanoparticulate Carrier for Oral Insulin Delivery. *Drug Delivery* 2008;15(2):127-139.

- 1
- 2
- 3 31. Azizi E, Namazi A, Haririan I, Fouladdel S, Khoshayand MR, Shotorbani PY, Nomani A, Gazori
- 4 T. Release profile and stability evaluation of optimized chitosan/alginate nanoparticles as
- 5 EGFR antisense vector. *International Journal of Nanomedicine* 2010;5:455-461.
- 6 32. Taqieddin E, Amiji M. Enzyme immobilization in novel alginate–chitosan core-shell
- 7 microcapsules. *Biomaterials* 2004;25(10):1937-1945.
- 8 33. Chandy T, Mooradian DL, Rao GH. Evaluation of modified alginate-chitosan-polyethylene
- 9 glycol microcapsules for cell encapsulation. *Artif Organs* 1999;23:894 - 903.
- 10 34. Klinkenberg G, Lystad KQ, Levine TDW, Dyrset N. Cell release from alginate immobilized
- 11 *Lactococcus lactis* ssp *lactis* in chitosan and alginate coated beads. *J Dairy Sci* 2001;84:1118 -
- 12 1127.
- 13 35. Bykowska A, Starosta R, Komarnicka UK, Ciunik Z, Kyzioł A, Guz-Regner K, Bugla-Płoskonska
- 14 G, Jezowska-Bojczuk M. Phosphine derivatives of ciprofloxacin and norfloxacin, a new class of
- 15 potential therapeutic agents. *New J. Chem.* 2014;38:1062-1071.
- 16 36. Hesse D, Ehlert N, Luenhop T, Smoczek A, Glage S, Behrens P, Muller PP, Esser KH, Lenarz T,
- 17 Stieve M and others. Nanoporous silica coatings as a drug delivery system for ciprofloxacin:
- 18 outcome of variable release rates in the infected middle ear of rabbits. *Otol Neurotol*
- 19 2013;34(6):1138-1145.
- 20 37. Venkatasubbu GD, Ramasamy S, Ramakrishnan V, Kumar J. Hydroxyapatite-alginate
- 21 nanocomposite as drug delivery matrix for sustained release of ciprofloxacin. *J Biomed*
- 22 *Nanotechnol* 2011;7(6):759-767.
- 23 38. Cipolla D, Blanchard J, Gonda I. Development of Liposomal Ciprofloxacin to Treat Lung
- 24 Infections. *Pharmaceutics* 2016;8(6):1-31.
- 25 39. Krajewska B, Wydro P, Jańczyk A. Probing the Modes of Antibacterial Activity of Chitosan.
- 26 Effects of pH and Molecular Weight on Chitosan Interactions with Membrane Lipids in
- 27 Langmuir Films. *Biomacromolecules* 2011;12:4144–4152.
- 28 40. Babic S, Horvat AJM, Mutavdzic Pavlovic D, Kastelan-Macan M. Determination of pKa values
- 29 of active pharmaceutical ingredients. *Trends in Analytical Chemistry* 2007;26(11):1043-1061.
- 30 41. Abdelwahed W, Degobert G, Stainmesse S, Fessi H. Freeze-drying of nanoparticles:
- 31 Formulation, process and storage considerations. *Advanced Drug Delivery Reviews*
- 32 2006;58:1688-1713.
- 33 42. Stippler E, Kopp S, Dressman JB. Comparison of US Pharmacopeia Simulated Intestinal Fluid
- 34 TS (without pancreatin) and Phosphate Standard Buffer pH 6.8, TS of the International
- 35 Pharmacopoeia with Respect to Their Use in In Vitro Dissolution Testing. *Dissolution*
- 36 *Technologies* 2004:7-10.
- 37 43. Motwani SK, Chopra S, Talegaonkar S, Kohli K, Ahmad FJ, Khar RK. Chitosan-sodium alginate
- 38 nanoparticles as submicroscopic reservoirs for ocular delivery: Formulation, optimisation and
- 39 *in vitro* characterisation. *European Journal of Pharmaceutics and Biopharmaceutics*
- 40 2008;68(3):513-525.
- 41 44. Oh N, Park JH. Endocytosis and exocytosis of nanoparticles in mammalian cells. *International*
- 42 *Journal of Nanomedicine* 2014;9(1):51-63.
- 43 45. Sarmiento B, Ribeiro A, Veiga F, Sampaio P, Neufeld R, Ferreira D. Alginate/chitosan
- 44 nanoparticles are effective for oral insulin delivery. *Pharm Res* 2007;12(2):198-206.
- 45 46. Ribeiro AJ, Silva C, Ferreira D, Vega F. Chitosan-reinforced alginate microspheres obtained
- 46 through the emulsification/internal gelation technique. *Eur. J. Pharm. Sci.* 2005;25:31-40.
- 47 47. Cheung RCF, Ng TB, Wong JH, Chan WY. Chitosan: An Update on Potential Biomedical and
- 48 Pharmaceutical Applications. *Mar. Drugs* 2015;13:5156-5186.
- 49 48. Borges O, Borchard G, Verhoef JC, de Sousa A, Junginger HE. Preparation of coated
- 50 nanoparticles for a new mucosal vaccine delivery system. *International Journal of*
- 51 *Pharmaceutics* 2005;299(1–2):155-166.
- 52 49. Bazban-Shotorbani S, Dashtimoghadam E, Karkhaneh A, Hasani-Sadrabadi MM, Jacob KI.
- 53 Microfluidic Directed Synthesis of Alginate Nanogels with Tunable Pore Size for Efficient
- 54 Protein Delivery. *Langmuir* 2016;32:4996–5003.
- 55
- 56
- 57
- 58
- 59
- 60

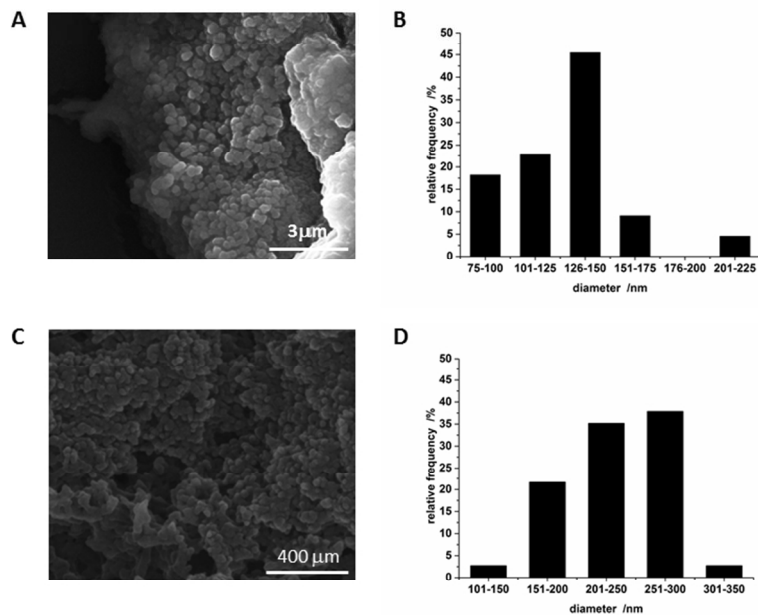
- 1
  - 2
  - 3
  - 4
  - 5
  - 6
  - 7
  - 8
  - 9
  - 10
  - 11
  - 12
  - 13
  - 14
  - 15
  - 16
  - 17
  - 18
  - 19
  - 20
  - 21
  - 22
  - 23
  - 24
  - 25
  - 26
  - 27
  - 28
  - 29
  - 30
  - 31
  - 32
  - 33
  - 34
  - 35
  - 36
  - 37
  - 38
  - 39
  - 40
  - 41
  - 42
  - 43
  - 44
  - 45
  - 46
  - 47
  - 48
  - 49
  - 50
  - 51
  - 52
  - 53
  - 54
  - 55
  - 56
  - 57
  - 58
  - 59
  - 60
50. Lucinda-Silva RM, Salgado HRN, Evangelista RC. Alginate–chitosan systems: In vitro controlled release of triamcinolone and in vivo gastrointestinal transit. *Carbohydrate Polymers* 2010;81:260-268.
51. Fonte P, Soares S, Costa A, Andrade JC, Seabra V, Reis S, Sarmento B. Effect of cryoprotectants on the porosity and stability of insulin-loaded PLGA nanoparticles after freeze-drying. *Biomatter* 2012;2(4):329-339.
52. Honary S, Zahir F. Effect of Zeta Potential on the Properties of Nano-Drug Delivery Systems - A Review. *Tropical Journal of Pharmaceutical Research* 2013;12(2):255-264.
53. Wang Q, Dong Z, Du Y, Kennedy JF. Controlled release of ciprofloxacin hydrochloride from chitosan/polyethylene glycol blend films. *Carbohydrate Polymers* 2007;69:336-343.
54. Li P, Dai YN, Zhang JP, Wang AQ, Wei Q. Chitosan-Alginate Nanoparticles as a Novel Drug Delivery System for Nifedipine. *Int J Biomed Sci* 2008;4(3):221-228.
55. Sarmento B, Ribeiro AJ, Veiga F, Ferreira DC, Neufeld RJ. Insulin-loaded nanoparticles are prepared by alginate ionotropic pre-gelation followed by chitosan polyelectrolyte complexation. *J Nanosci Nanotechnol* 2007;7:2833-2841.
56. Hari PR, Chandy T, Sharma CP. Chitosan/calcium–alginate beads for oral delivery of insulin. *J Appl Polym Sc* 1996;56:1795-1801.
57. Janes KA, Calvo P, Alonso MJ. Polysaccharide colloidal particles as delivery systems for macromolecules. *Advanced Drug Delivery Reviews* 2001;47(1):83-97.
58. Tapia C, Molina S, Diaz A, Abugoch L, Diaz-Dosque M, Valenzuela F, Yazdani-Pedram M. The Effect of Chitosan as Internal or External Coating on the 5-ASA Release from Calcium Alginate Microparticles. *AAPS PharmSciTech*, Vol. 11, No. 3, September 2010;11(3):1294-1305.
59. Simonoska Crcarevska M, Glavas Dodov M, Goracinova K. Chitosan coated Ca-alginate microparticles loaded with budesonide for delivery to the inflamed colonic mucosa. *Eur J Pharm Biopharm* 2008;68(3):565-578.
60. Costa P, Lobo JM. Modeling and comparison of dissolution profiles. *European Journal of Pharmaceutical Sciences* 2001;13:123-133.
61. Dash S, Murthy APN, Nath L, Chowdhury P. Kinetic modeling on drug release from controlled drug delivery systems. *Acta Poloniae Pharmaceutica - Drug Research* 2010;67(3):217-223.





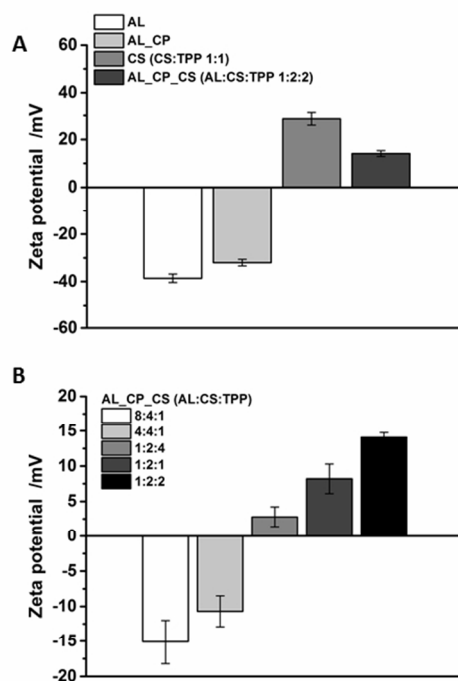
The mean hydrodynamic diameter determined by NTA for AL\_CP and AL\_CP\_CS formulations.

296x209mm (300 x 300 DPI)



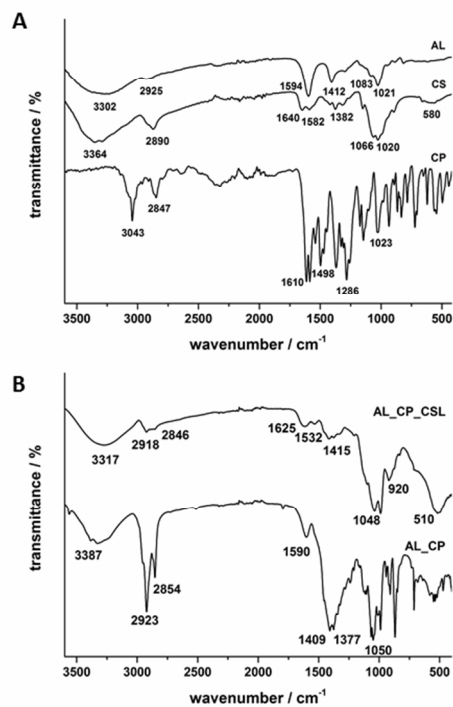
SEM image of the AL\_CP (A) and AL\_CP\_CS (C) particles with the corresponding size distribution (ImageJ) for AL\_CP (B) and AL\_CP\_CS (D), respectively.

254x190mm (96 x 96 DPI)



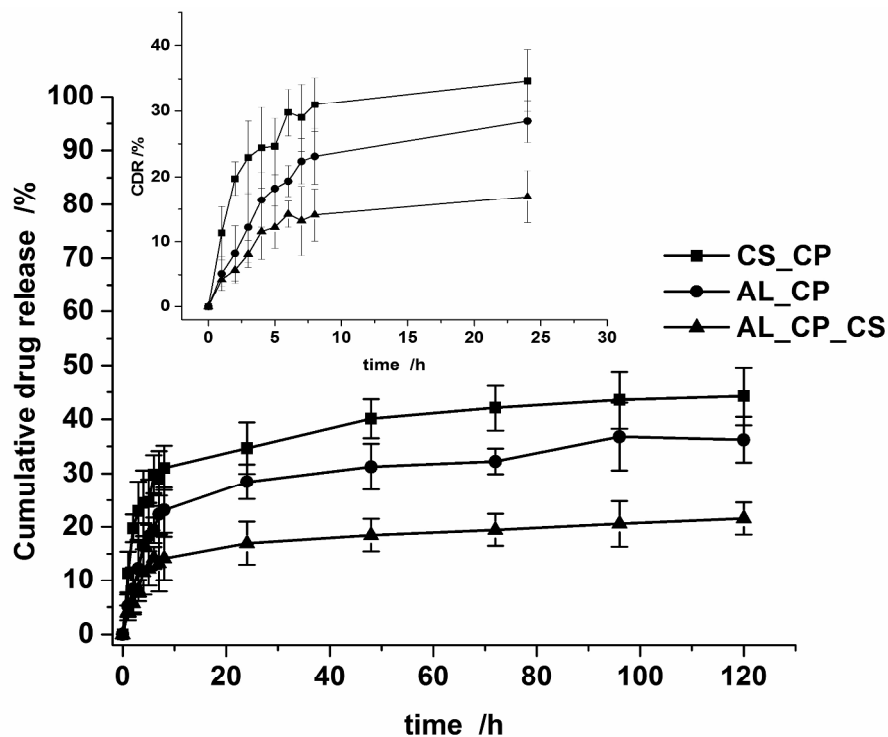
Zeta potential dependency on formulation content (A) and the weight ratio of particular polymers and TPP (B) in pH = 6.0.

254x190mm (96 x 96 DPI)



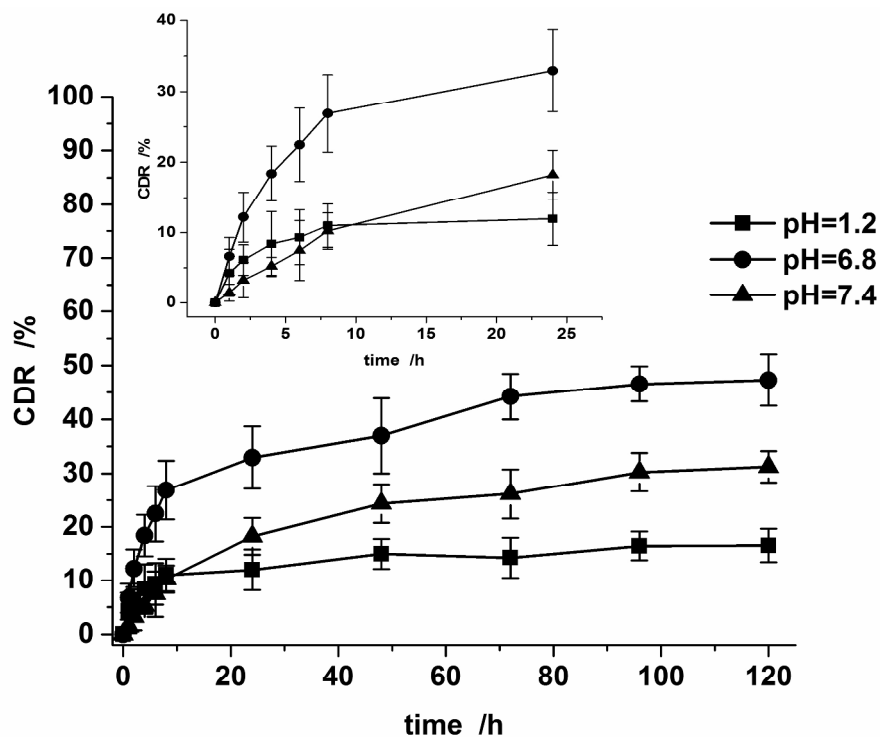
FTIR spectra of AL, CS, and CP (A), and AL\_CP and AL\_CP\_CS (B).

254x190mm (96 x 96 DPI)



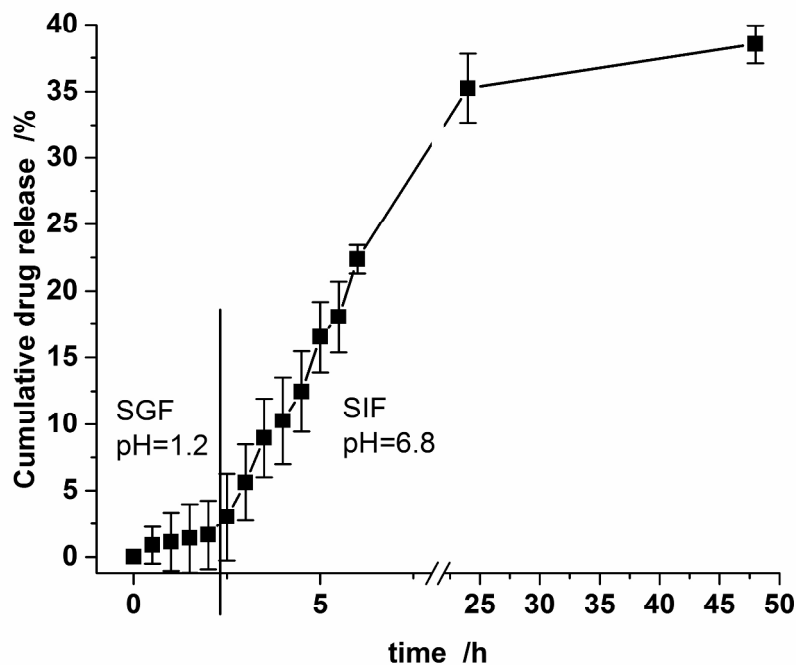
Kinetic curves of ciprofloxacin release over time in aqueous media at 37°C from the CS\_CP (■), AL\_CP (●), and AL\_CP\_CS (▲) formulations. Inset: magnification of release time scale (from 0 to 24 hours).

272x208mm (300 x 300 DPI)



Kinetic curves of ciprofloxacin release over time from the AL\_CS\_CP formulations in different pH = 1.2 (■), pH = 6.8 (●), and pH = 7.4 (▲) at 37°C. Inset: magnification of release time scale (from 0 to 24 hours).

272x208mm (300 x 300 DPI)



The kinetic curve of ciprofloxacin release over time from the AL\_CS\_CP formulations firstly in pH =1.2 and then continued in pH = 6.8 at 37°C.

272x208mm (300 x 300 DPI)

**TABLE 1** Correlation coefficients for different mathematical models applied on the release kinetics from the AL\_CS\_CP formulations in different pHs.

Kinetic model	Correlation coefficient ( $R^2$ ) <sup>a</sup>		
	pH = 1.2	pH = 6.8	pH = 7.4
Zero order	0.9412	0.9489	0.9841
First order	0.9462	0.9645	0.9840
Higuchi	<b>0.9856</b>	<b>0.9910</b>	0.9713
Hixson-Crowell	0.9446	0.9596	0.9841
Korsmeyer-Peppas (n) <sup>b</sup>	<b>0.9894</b> (0.44)	0.9778 (0.64)	<b>0.9892</b> (0.89)

<sup>a</sup> Bold values indicate the best fits

<sup>b</sup> Release exponent (n) evaluated for <60% of drug release